Supplementary Information

Disentangling nanoscale electric and magnetic fields by time-reversal operation in differential phase-contrast STEM.

M. Campanini,[1]* L.Nasi,[2] F. Albertini[2], R. Erni[1]

[1]*Electron Microscopy Center, Empa – Swiss Federal Laboratories for Materials Science and Technology, Ueberlandstrasse 129, 8600 Duebendorf, Switzerland*
[2]*Istituto dei Materiali per l'Elettronica ed il Magnetismo, IMEM-CNR, Parco delle Scienze 37/A, 43124 Parma, Italy*

*Author to whom correspondence should be addressed: marco.campanini@empa.ch

S1. Experimental settings for ADF and DPC imaging

The experiments were performed using an FEI Titan Themis operated at 300 kV, in Lorentz STEM mode.
The ADF signal was recorded setting the camera length to 9.1 m, for which the angular range of the annular detector is 0.21 – 0.84 mrad. The DPC measurement was performed by setting the camera length to 19 m, for which the angular range of the segmented detector spans from about 0.1 to 0.4 mrad.

S2. DPC signal normalization

The differential phase-contrast (DPC) scanning transmission electron microscopy (STEM) signals can be affected by local changes in the thickness, density, or composition of the specimen, as they may induce a change in the total intensity of the diffraction pattern. The differential signals obtained calculating the difference between the intensity detected by opposite quadrants need to be normalized to correct for such absorption of diffraction effects for the proper detection of the specimen's electric and magnetic fields.
As proposed by F. Schwarzhuber et al.,[1] a convenient way for normalizing the differential signals is to divide the DPC signal vector by the position-dependent signal sum, obtained by summing the intensities of the 4 quadrants (A, B, C, D).For the probe position $\mathbf{r_P}$ (in the specimen plane) such sum reads:

$$\mathrm{S_{sum}}(\mathbf{r_P}) = \sum_{\mathrm{seg=A}}^{D} \mathrm{I}(\mathbf{r_P}) \qquad \text{Eq. 1}$$

We can define the DPC signal vector as:

$$\vec{\mathrm{S}}_{\mathrm{DPC}}(\mathbf{r_P}) = \vec{\mathrm{I}}_{\mathrm{A-C}}(\mathbf{r_P}) + \vec{\mathrm{I}}_{\mathrm{B-D}}(\mathbf{r_P}) \qquad \text{Eq. 2}$$

where $\vec{\mathrm{I}}_{\mathrm{A-C}}(\mathbf{r_P}) = \mathrm{I_A}(\mathbf{r_P}) - \mathrm{I_C}(\mathbf{r_P})$ and $\vec{\mathrm{I}}_{\mathrm{B-D}}(\mathbf{r_P}) = \mathrm{I_B}(\mathbf{r_P}) - \mathrm{I_D}(\mathbf{r_P})$.
The normalization of the DPC images is thus defined by the following relation:

$$\frac{\vec{\mathrm{S}}_{\mathrm{DPC}}}{\mathrm{S_{sum}}} = \frac{\vec{\mathrm{I}}_{\mathrm{A-C}}}{\mathrm{S_{sum}}} + \frac{\vec{\mathrm{I}}_{\mathrm{B-D}}}{\mathrm{S_{sum}}} \equiv [(\mathrm{A-C})_n\,, (\mathrm{B-D})_n] \qquad \text{Eq. 3}$$

The DPC signals – i.e. $(\mathrm{A\text{-}C})_n$ and $(\mathrm{B\text{-}D})_n$ – shown in Fig. 1 in the manuscript were obtained applying such a normalization procedure.

Following the argumentations in Ref. [1], it is straightforward to prove that the normalized DPC signal vector is related to the projected electric field and magnetic field.
For the probe position $\mathbf{r_P}$, in fact, the beam deflection detected by DPC can be related to an electric field by the equation:

$$\frac{\vec{\mathrm{S}}_{\mathrm{DPC}}(\mathbf{r_P})}{\mathrm{S_{sum}}(\mathbf{r_P})} = \frac{1}{\kappa_{\mathrm{el}}} \int_{-\infty}^{+\infty} \vec{\mathrm{E}}\,(\mathbf{r_P})\,\mathrm{dz} \qquad \text{Eq. 4}$$

or to a magnetic field by the expression:

$$\frac{\vec{S}_{DPC}(\mathbf{r_P})}{S_{sum}(\mathbf{r_P})} = \frac{1}{\kappa_{mag}} \int_{-\infty}^{+\infty} \nabla A_z(\mathbf{r_P})\, dz \qquad \text{Eq. 5}$$

where the two factors κ_{el} and κ_{mag} are given respectively by:

$$\kappa_{el} = \frac{R^2 - r^2}{R \cdot C} \frac{m_{rel} v_{rel}^2}{e} \qquad \text{Eq. 6}$$

$$\kappa_{magn} = \frac{R^2 - r^2}{R \cdot C} \frac{m_{rel} v_{rel}}{e} \qquad \text{Eq. 7}$$

with R and r being respectively the radii of the diffraction disk and the detector hole, C the camera length, m_{rel} and v_{rel} the relativistic electron mass and velocity, e the electron charge.
In the most complex case, the DPC signal vector will be the sum of the two contributions expressed by the Eq. 4 and 5. It is worth noting that for given experimental settings the two factors κ_{el} and κ_{mag} are different. Indeed, this highlights the importance of the separation procedure for the qualitative interpretation of the data, being the electrostatic contribution to the beam deflection amplified with respect to the magnetic one.

Finally, we can show that the DPC signal so calculated is a valid approximation of the center-of-mass measurement. In particular, under the phase object approximation, we can write the center-of-mass (COM) as a function of the gradient of the phase shift of the electron wave as it travels through the sample:[2]

$$\vec{COM}(\mathbf{r_P}) = \frac{1}{2\pi} I_P(\mathbf{r}) \star \nabla\phi(\mathbf{r}) \qquad \text{Eq. 8}$$

where I_P is the probe intensity, ϕ is the phase shift, and $\mathbf{r}$ is the coordinate in the specimen plane.
Since the phase shift induced by the specimen's electric and magnetic field can be written as:

$$\phi(\mathbf{r}) = \phi_{el}(\mathbf{r}) + \phi_{mag}(\mathbf{r}) = \frac{e}{\hbar v} \int_{-\infty}^{+\infty} V(\mathbf{r})\, dz - \frac{e}{\hbar} \int_{-\infty}^{+\infty} A_z(\mathbf{r})\, dz \qquad \text{Eq. 9}$$

with V the electrostatic potential and A_z the component of the magnetic potential parallel to the electron beam, the center-of-mass is equal to:

$$\vec{COM}(\mathbf{r_P}) = \frac{1}{2\pi} I_P(\mathbf{r}) \star \left[\frac{e}{\hbar v} \int_{-\infty}^{+\infty} \nabla V(\mathbf{r})\, dz - \frac{e}{\hbar} \int_{-\infty}^{+\infty} \nabla A_z(\mathbf{r})\, dz \right] \qquad \text{Eq. 10}$$

The center-of-mass components along the two main directions are thus given by:

$$COM_x(\mathbf{r_P}) = -\frac{e}{h} I_P(\mathbf{r}) \star \left[\frac{1}{v} \int_{-\infty}^{+\infty} E_x(\mathbf{r})\, dz - \int_{-\infty}^{+\infty} B_y(\mathbf{r})\, dz \right] \qquad \text{Eq. 11}$$

$$COM_y(\mathbf{r_P}) = -\frac{e}{h} I_P(\mathbf{r}) \star \left[\frac{1}{v} \int_{-\infty}^{+\infty} E_y(\mathbf{r}) dz + \int_{-\infty}^{+\infty} B_x(\mathbf{r})\, dz \right] \qquad \text{Eq. 12}$$

where we used the definition of the electric field:

$$\nabla\phi(\mathbf{r}) = \vec{E}(\mathbf{r}) = [E_x, E_y] \qquad \text{Eq. 13}$$

and the definition of the magnetic vector potential:

$$\vec{B}(\mathbf{r}) = \nabla \times A_z(\mathbf{r}) = \left[\frac{d}{dy} A_z(\mathbf{r}), -\frac{d}{dx} A_z(\mathbf{r}) \right] \qquad \text{Eq. 14}$$

It is straightforward to observe that the DPC components previously defined correspond to an approximation to the center-of-mass measurement. Assuming in fact that the segments A and C are along the *x*-axis and, correspondingly, the segments B and D along the *y*-axis, we obtain:

$$(A - C)_n = \frac{1}{\kappa_{el}} \int_{-\infty}^{+\infty} E_x(\mathbf{r_P}) dz - \frac{1}{\kappa_{mag}} \int_{-\infty}^{+\infty} B_y(\mathbf{r_P})\, dz \qquad \text{Eq. 15}$$

$$(\mathrm{B}-\mathrm{D})_{\mathrm{n}}=\frac{1}{\kappa_{\mathrm{el}}}\int_{-\infty}^{+\infty}\mathrm{E}_{y}\left(\mathbf{r}_{\boldsymbol{P}}\right)\mathrm{dz}+\frac{1}{\kappa_{\mathrm{mag}}}\int_{-\infty}^{+\infty}B_{x}\left(\mathbf{r}_{\boldsymbol{P}}\right)\,\mathrm{dz} \qquad \text{Eq. 16}$$

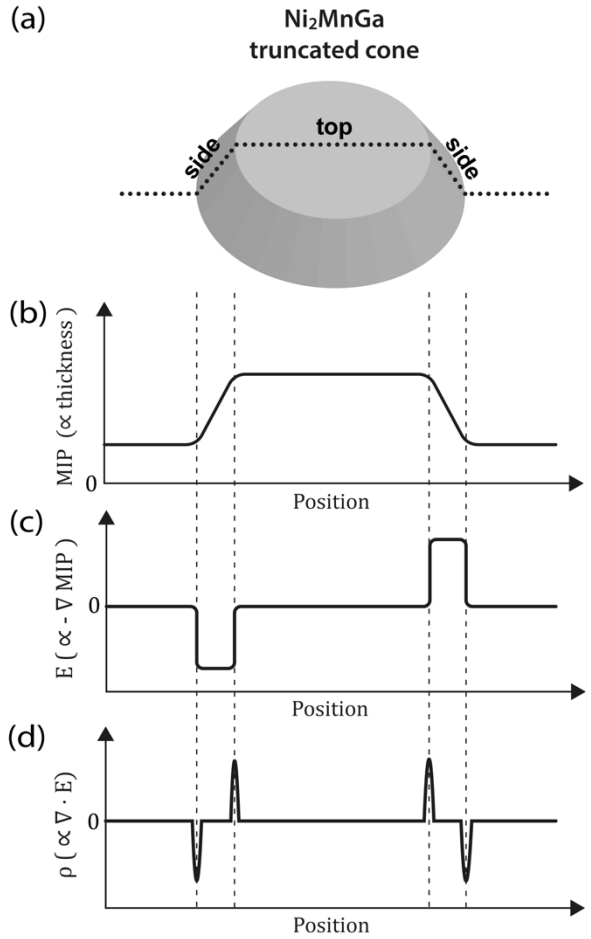

Fig. S3. (a) The Ni_2MnGa disk has a shape of a truncated cone. The dashed line gives the direction of the line profiles. (b) Due to the uniform specimen composition, the line-profile of the mean inner potential is proportional to the specimen thickness. (c) The electric field (proportional to the gradient of the mean inner potential) shows a non-zero signal at the two sides of the disk, where a thickness variation is observed. (c) Similarly, opposite charges are observed at the two extreme points of the sides of the truncated cone.

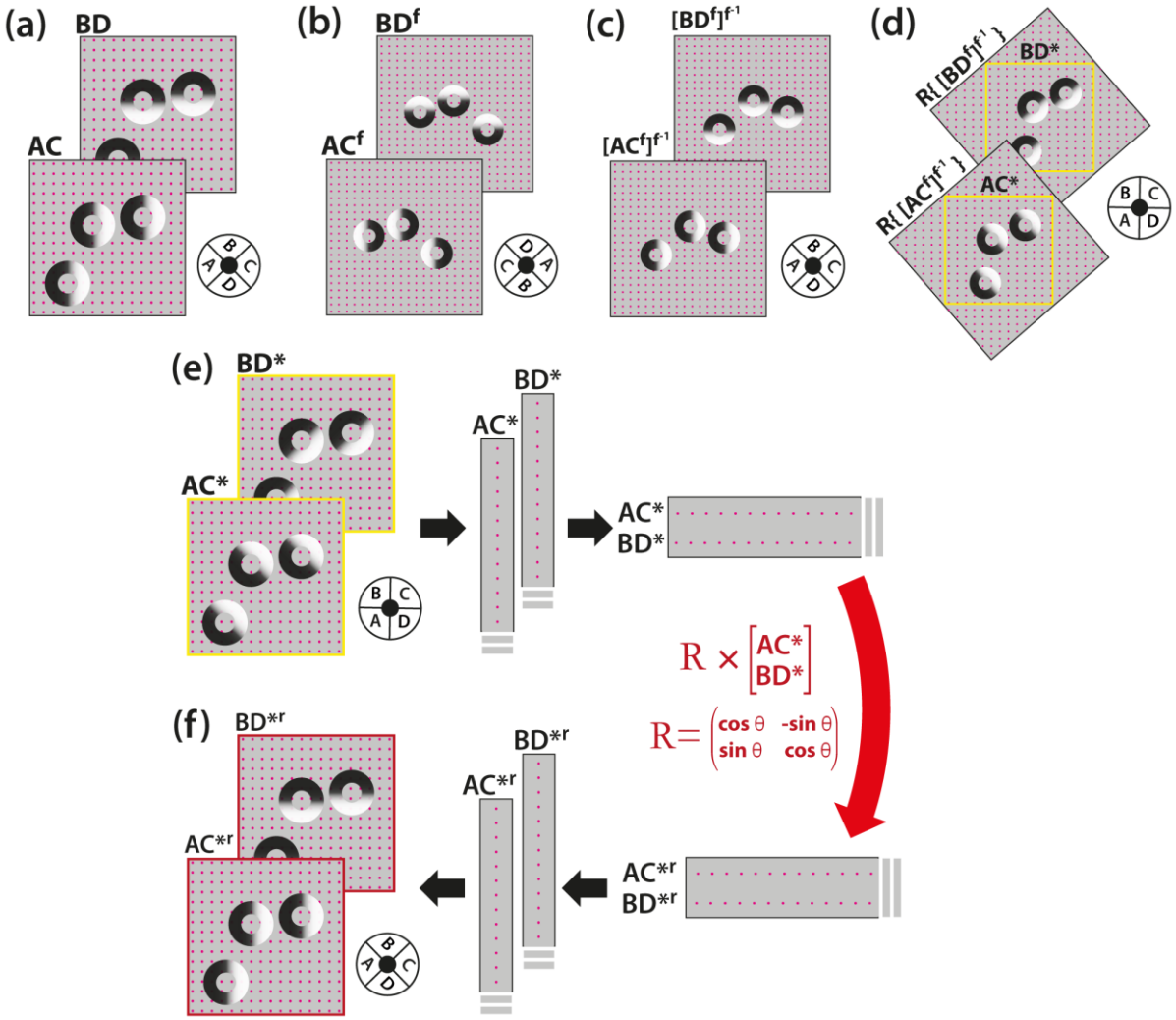

Fig. S4. Scheme of the alignment and re-calculation processes applied in the separation experiment. (a) Experimental direct DPC signals. (b) DPC signal obtained after flipping the specimen. A finite rotation of the specimen is also intentionally introduced to match the real experimental case. The scan area is chosen slightly larger than the field of view of the direct experiment for allowing the image alignment procedures. (c) DPC signals shown in (b) are flipped back to match the direct experiment specimen. (d) The DPC signals so obtained are finally rotated and aligned to the direct DPC signals. The signals (AC*, BD*) cover the same field of view of (AC, BD) and they have the same magnification. However, the DPC main axes in (AC*, BD*) are at an angle with respect to the ones of (AC, BD). (e) A vector rotation – given by the rotation matrix R – of the DPC axes is then performed and allows to obtain a signal (AC^{*r}, BD^{*r}) that can be summed/subtracted to (AC, BD) for the separation procedure.

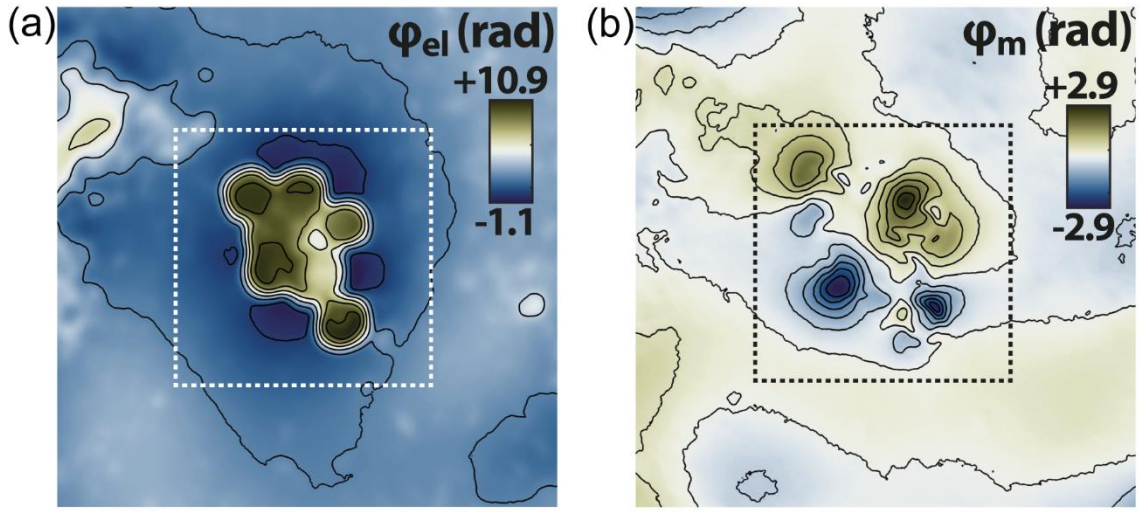

Fig. S5 (a) Electrostatic phase shift and (b) magnetic phase shift as obtained after applying the separation procedure. The phase contours are also plot overlaid to the maps. The area corresponding to the field of view of Fig. 3 (c-f) is marked by the dashed box.

References

[1] F. Schwarzhuber, P. Melzl, and J. Zweck, Ultramicroscopy **177**, 97 (2017).
[2] I. Lazić, E.G.T. Bosch, and S. Lazar, Ultramicroscopy **160**, 265 (2016).